Monthly Notices
of the
ROYAL ASTRONOMICAL SOCIETY

Mon. Not. R. Astron. Soc. **406,** 1959–1966 (2010) doi:10.1111/j.1365-2966.2010.16801.x

Constraints on black hole duty cycles and the black hole–halo relation from SDSS quasar clustering

Francesco Shankar,[1⋆] David H. Weinberg[2,3] and Yue Shen[4,5]

[1]*Max-Planck-Institüt für Astrophysik, Karl-Schwarzschild-Str. 1, D-85748 Garching, Germany*
[2]*Astronomy Department and Center for Cosmology and Astro-Particle Physics, Ohio State University, Columbus, OH-43210, USA*
[3]*Institute for Advanced Study, Princeton, NJ-08540, USA*
[4]*Princeton University Observatory, Princeton, NJ-08544, USA*
[5]*Harvard-Smithsonian Center for Astrophysics, Cambridge, MA-02138, USA*

Accepted 2010 April 7. Received 2010 February 9; in original form 2009 August 5

ABSTRACT

We use Shen et al.'s (2009) measurements of luminosity-dependent clustering in the Sloan Digital Sky Survey Data Release 5 quasar catalogue, at redshifts $0.4 \leq z \leq 2.5$, to constrain the relation between quasar luminosity and host halo mass and to infer the duty cycle $f_{\rm opt}$, the fraction of black holes that shine as optically luminous quasars at a given time. We assume a monotonic mean relation between quasar luminosity and host halo mass, with lognormal scatter Σ. For specified $f_{\rm opt}$ and Σ, matching the observed quasar space density determines the normalization of the luminosity–halo mass relation, from which we predict the clustering bias. The data show no change of bias between the faint and bright halves of the quasar sample but a modest increase in bias for the brightest 10 per cent. At the mean redshift $z = 1.45$ of the sample, the data can be well described either by models with small intrinsic scatter ($\Sigma = 0.1$ dex) and a duty cycle $f_{\rm opt} = 6 \times 10^{-4}$ or by models with much larger duty cycles and larger values of the scatter. 'Continuity equation' models of the black hole mass population imply $f_{\rm opt} \geq 2 \times 10^{-3}$ in this range of masses and redshifts, and the combination of this constraint with the clustering measurements implies scatter $\Sigma \geq 0.4$ dex. These findings contrast with those inferred from the much stronger clustering of high-luminosity quasars at $z \approx 4$, which require minimal scatter between luminosity and halo mass and duty cycles close to one.

Key words: galaxies: active – galaxies: evolution – quasars: general – cosmology: theory.

1 INTRODUCTION

The strong correlations between the masses of central black holes (BHs) and the luminosities, dynamical masses and velocity dispersions σ of their host galaxies imply that the growth processes of BHs and their hosts are intimately linked (e.g. Magorrian et al. 1998; Ferrarese & Merritt 2000; Gebhardt et al. 2000; Ferrarese 2002; Ferrarese & Ford 2005; Graham 2007; Tundo et al. 2007; Shankar, Bernardi & Haiman 2009b). However, constraining the cosmological evolution of BHs remains a challenge. Although a variety of theoretical models may roughly match observations, the underlying physical assumptions on BH growth can vary drastically from one model to another (e.g. Sołtan 1982; Silk & Rees 1998; Salucci et al. 1999; Cavaliere & Vittorini 2000; Kauffmann & Haehnelt 2000; Yu & Tremaine 2002; Steed & Weinberg 2003; Wyithe & Loeb 2003; Granato et al. 2004, 2006; Marconi et al. 2004; Merloni, Rudnick & Di Matteo 2004; Yu & Lu 2004; Miralda-Escudé & Kollmeier 2005; Murray, Quataert & Thompson 2005; Cattaneo et al. 2006; Croton et al. 2006; Hopkins et al. 2006; Lapi et al. 2006; Shankar et al. 2004, 2006; Malbon et al. 2007; Monaco, Fontanot & Taffoni 2007; Croton 2009; Cook, Lapi & Granato 2009; Shankar, Weinberg & Miralda-Escudé 2009a). Quasar clustering provides additional, independent constraints on the BH population, helping to discriminate among otherwise viable models. As outlined by Martini & Weinberg (2001) and Haiman & Hui (2001; see also Wyithe & Loeb 2005; Lidz et al. 2006; Hopkins et al. 2007; Shankar & Mathur 2007; White, Martini & Cohn 2008; Shen et al. 2009a,b; Shankar et al. 2009c; Wyithe & Loeb 2009; Bonoli et al. 2010), the clustering is an indirect measure of the masses, and therefore number densities, of the haloes hosting the quasars. In turn, the ratio between the quasar luminosity function and the halo mass function provides information on the duty cycle, i.e. the fraction of haloes that host active quasars at a given time. In general terms, stronger clustering implies that quasars reside in rarer, more massive hosts, and matching the observed quasar space density then requires a higher duty cycle.

In this paper, we model Shen et al.'s (2009a, hereafter S09) recent measurements of luminosity-dependent quasar clustering derived from the quasar redshift survey (Schneider et al. 2007) of the Sloan

⋆E-mail: shankar@mpa-garching.mpg.de

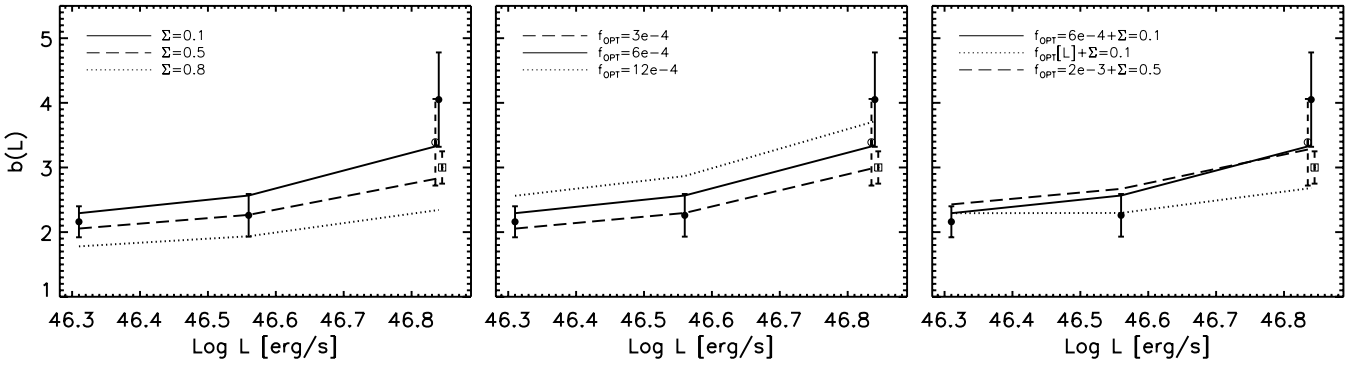

Figure 1. Bias as a function of bolometric luminosity. In all panels, the solid circles are the mean bias measured by S09 from the quasar autocorrelation function for the faint, bright and brightest subsamples in their analysis. The open circle with dashed error bars is the bias measured for the brightest subsample including in the fits the bins with negative correlation function. The open square is the bias computed from the cross-correlation of the most luminous sources with the rest of the sample. The data are compared with predictions of several models for the mean bias at $z = 1.45$, the average redshift of the S09 sample. Left-hand panel: comparison among models with the same value for the duty cycle $f_{\rm opt} = 6 \times 10^{-4}$ and different values of the intrinsic Gaussian scatter Σ (in dex) in the quasar luminosity–host halo relation, as labelled. Central panel: comparison among models with the same scatter $\Sigma = 0.1$ dex but different values of the duty cycle $f_{\rm opt}$, as labelled. Right-hand panel: comparison among three different models: one with constant $f_{\rm opt} = 6 \times 10^{-4}$ at all luminosities and scatter $\Sigma = 0.1$ (solid line); another with equal scatter but with a decreasing duty cycle $f_{\rm opt} = 6 \times 10^{-4}$ at $\log(L/{\rm erg\,s^{-1}}) = 46.31$, and $f_{\rm opt}/2$ and $f_{\rm opt}/4$ at $\log(L/{\rm erg\,s^{-1}}) = 46.56$ and 46.84, respectively (dotted line) and finally a model with $f_{\rm opt} = 2 \times 10^{-3}$ and $\Sigma = 0.5$ (long-dashed line).

Digital Sky Survey (SDSS; York et al. 2000) Data Release 5 (DR5; Adelman-McCarthy et al. 2007). Ross et al. (2009) also analyse the clustering of this quasar survey, concentrating on redshift evolution, but here we focus on the S09 results because they isolate the luminosity dependence of clustering. Our aim is to answer basic questions about the evolution of the active galactic nucleus (AGN) and supermassive BH population at $z \leq 2.5$. Does the duty cycle depend on quasar luminosity and/or redshift? What is the underlying relation between quasar luminosity and halo mass? Does it have scatter? More generally, what combinations of duty cycle and scatter are allowed by the measurements?

Throughout the paper, we adopt $\Omega_{\rm m} = 0.26$, $\Omega_\Lambda = 0.74$, $h \equiv H_0/100\,{\rm km\,s^{-1}\,Mpc^{-1}} = 0.7$, $\Omega_{\rm b} = 0.0435$, $n_{\rm s} = 0.95$, $\sigma_8 = 0.78$ and the transfer function of Eisenstein & Hu (1999; with zero neutrino contribution), which matches the cosmology used by S09.

2 DATA

The sample used by S09 is a homogeneous subset of a catalogue of 77 429 spectroscopically identified quasars brighter than $M_i = -22$, in the redshift range $0.1 \lesssim z \lesssim 5.0$. Shen et al. (2007) computed the correlation function of the high-redshift quasars at $z \geq 2.9$, modelled subsequently by White et al. (2008) and Shankar et al. (2009c). Here, instead we focus on the correlation function of lower redshift quasars in the range $0.4 \leq z \leq 2.5$. To probe the luminosity dependence of the bias, S09 divided the low-z sample into subsamples containing the fainter half of the quasars, the brighter half of the quasars and the brightest 10 per cent of the quasars (see their Fig. 2). In each luminosity bin, they computed the quasar correlation function. In particular, S09 estimated for the full sample a mean clustering bias of $b = 2.16 \pm 0.24$, 2.26 ± 0.33, 4.05 ± 0.73 for the faint, bright and brightest subsamples, with median luminosity $\log L_{\rm med}/{\rm erg\,s^{-1}} = 46.31$, 46.56, 46.84, respectively.[1] We will first compare with their data on the bias by computing models at the average redshift $z = 1.45$ of their sample (Fig. 1). We will then compute the full correlation functions for the faint, bright and brightest subsamples averaged over the full redshift distribution of the sample, and compare them with the S09 measurements (Fig. 2).

3 METHOD

By imposing a cumulative match between the space densities of quasars and their host haloes, and assuming that only a fraction $f_{\rm opt}$ of haloes of a given mass shine as optical quasars at a given time, we can estimate the mean host halo mass given the observed number density of quasars. Formally, this concept reads as (e.g. White et al. 2008)

$$\int_{x_{\rm min}}^{\infty} n(x,z){\rm d}x = \int_{-\infty}^{\infty} {\rm d}y f_{\rm opt}\Phi(y,z) \times \frac{1}{2}{\rm erfc}\left[\ln\left(\frac{10^{y_{\rm min}(x_{\rm min})}}{10^{y}}\right)\frac{1}{\sqrt{2}\ln(10)\Sigma}\right], \quad (1)$$

with $x = M_i(z = 2)$ and $y = \log M$. Here $\Phi(y, z)$ is the comoving number density of haloes, in units of ${\rm Mpc^{-3}\,dex^{-1}}$ for $H_0 = 70\,{\rm km\,s^{-1}\,Mpc^{-1}}$, which we take from Sheth & Tormen (1999), while $n(x, z)$ is the comoving number density of quasars (in ${\rm Mpc^{-3}}$) with absolute magnitude in the range $x \rightarrow x + {\rm d}x$. We take the observed luminosity function $n(x, z)$ from Richards et al. (2006), corrected to our cosmology. The quantity $f_{\rm opt}$ in equation (1) is the duty cycle, i.e. the fraction of haloes that host quasars shining above a minimum luminosity $x_{\rm min} = M_{i,{\rm min}}$ at redshift z. Equation (1) also takes into account a lognormal scatter with dispersion Σ (in dex) around the mean quasar luminosity–halo mass relation.[2] This scatter includes both the scatter between BH mass and halo mass and the scatter between luminosity and BH mass (i.e. in the Eddington ratio), and our analysis does not distinguish the two contributions.

[1] We here use the S09 conversion to bolometric luminosities $L = 10^{[M_i(z=2)-90]/(-2.5)}$, with $M_i(z = 2) = M_i(z = 0) - 0.596$, the i band, $z = 2$ K-corrected magnitude system introduced by Richards et al. (2006).

[2] Note that when comparing with the S09 measurements, equation (1) should have an upper limit on the left-hand side corresponding to the maximum luminosity $M_{i,{\rm max}}$ considered in the clustering measurement of a given subsample. However, we have checked that, as long as the right-hand side also has a similar cut-off in halo masses above the halo mass corresponding to $M_{i,{\rm max}}$, our results do not change.

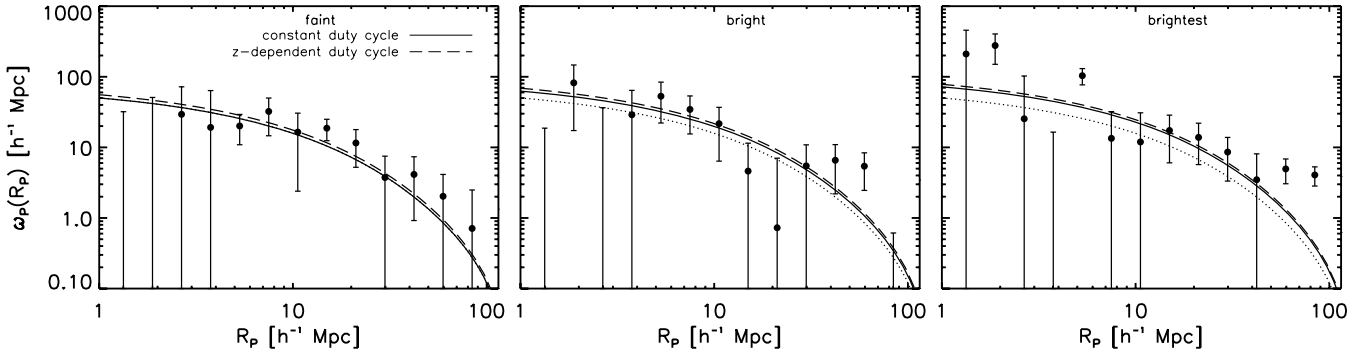

Figure 2. The projected correlation functions from S09 (solid points with error bars) are compared with the predictions of the low-scatter model from Fig. 1. The left-hand, middle and right-hand panels refer to the faint, bright and brightest subsamples (with the cross-correlation shown for the brightest sample). The solid lines refer to a model with constant duty cycle $f_{\rm opt} = 6 \times 10^{-4}$ at all luminosities and redshifts, while the long-dashed lines refer to a model with a redshift-dependent duty cycle $f_{\rm opt} = 6 \times 10^{-4} \times (1 + z/2.45)^8$. The predictions of the constant duty cycle model for the faint sample are also shown as dotted lines in the last two panels for comparison.

At each redshift, equation (1) defines the minimum halo mass $y_{\rm min}$ corresponding to the minimum luminosity in the sample $x_{\rm min}$ (the latter taken from S09). We then compute the mean bias $\bar{b}$ associated to a given subsample at redshift z with *median* luminosity $\langle x \rangle = M_{i,\rm med}$ and minimum luminosity $x_{\rm min}$ as

$$\bar{b}_{\langle x \rangle}(z) = \frac{\int_0^\infty {\rm d}y \Phi(y, z) W[y_{\rm min}(x_{\rm min}), y] b(y, z)}{\int_0^\infty {\rm d}y \Phi(y, z) W[y_{\rm min}(x_{\rm min}), y]}, \quad (2)$$

with

$$W[y_{\rm min}(x_{\rm min}), y] = {\rm erfc}\left[\ln\left(\frac{10^{y_{\rm min}(x_{\rm min})}}{10^y}\right)\frac{1}{\sqrt{2}\ln(10)\Sigma}\right] \quad (3)$$

and $b(y, z)$ the halo bias given by Sheth, Mo & Tormen (2001). We stress here that an upper luminosity limit to the bin, corresponding to an upper cut in halo mass (see footnote 2), does not significantly alter the expected bias given by equation (2).

To perform a detailed comparison with the S09 data, for at least some of the models discussed below, we also compute the quasar auto- and cross-correlation functions for each of S09's redshift and luminosity bins. The quasar autocorrelation function is given by

$$\xi(R, z) = D^2(z)\bar{b}^2_{\langle x \rangle}(z)\xi_m(R), \quad (4)$$

where $D(z)$ is the linear growth factor of perturbations and $\xi_m(R)$ is the linear matter correlation function at $z = 0$ derived from the power spectrum. To compute the cross-correlation function and to compare with the S09 10 per cent most luminous quasars, we instead use the relation

$$\xi_{\rm cross}(R, z) = D^2(z)\bar{b}_{\rm brightest}\bar{b}_{\rm faint}\xi_m(R), \quad (5)$$

where $\bar{b}_{\rm brightest}$ is the bias associated to the most luminous quasars, while $\bar{b}_{\rm faint}$ is the average bias associated to the faintest luminosity in the sample at the same redshift.

We then convert the autocorrelation function into a projected correlation function via the relation

$$w_{\rm P}(R_{\rm P}, z) = 2\int_0^\infty {\rm d}R_z\, \xi\left(R = \sqrt{R_{\rm P}^2 + R_z^2}, z\right). \quad (6)$$

Finally, we compute the average projected correlation function by weighting with the quasar number redshift distribution $N(z)$ and volumes probed in each bin considered as

$$w_{\rm P}(R_{\rm P}) = \frac{\int {\rm d}z\, ({\rm d}V/{\rm d}z)\, N^2(z) w_{\rm P}(R_{\rm P}, z)}{\int {\rm d}z\, ({\rm d}V/{\rm d}z)\, N^2(z)}. \quad (7)$$

By comparing the bias and the average projected correlation function with the data, we can extract useful information on the underlying duty cycle $f_{\rm opt}$ and scatter Σ. We have checked that including subhaloes as quasar hosts, with the methods of Giocoli et al. (2007), does not noticeably alter our predicted quasar bias or correlation function, because the abundance of massive subhaloes is very small compared to the abundance of haloes above the minimum halo masses probed here.

4 RESULTS

4.1 Clustering constraints on duty cycle and scatter

Fig. 1 compares the bias factor predicted by several illustrative models to the values inferred by S09 from the quasar correlation function for the faint, bright and brightest subsamples, shown by the solid circles. At each redshift, these subsamples contain the fainter half, brighter half and brightest 10 per cent of the quasars above the SDSS magnitude threshold. The open square shows the bias factor inferred from the cross-correlation of the brightest sample with the remaining quasars. The open circle with dashed error bars shows the bias measured for the brightest subsample (derived by S09 directly from the cross-correlation function using their equation 3) when negative correlation function points are included in the bias fit. As discussed by S09, it is unclear whether the negative points are purely statistical fluctuations or artefacts of the redshift variation of quasar selection efficiency, so there is some ambiguity about whether it is more accurate to retain or omit these data points. This question should be resolved by the larger data sample from the final SDSS data release, which will have smaller statistical fluctuations. Nevertheless, we will show below that our main conclusions hold irrespective of the exact data set considered.

Lines in Fig. 1 show model predictions for a variety of assumptions. By applying equations (1) and (2) we compute the mean bias as a function of bolometric luminosity at the single redshift $z = 1.45$, the mean redshift of the S09 sample, for different input duty cycle $f_{\rm opt}$ and scatter Σ. The solid line in the left-hand panel shows a reference model consistent with the data on the bias, defined by a small scatter $\Sigma = 0.1$ dex and a constant duty cycle $f_{\rm opt} = 6 \times 10^{-4}$. As expected, increasing the scatter to e.g. $\Sigma = 0.5$, 0.8, lowers the predicted bias and flattens the relation between bias and luminosity (long-dashed and dotted lines), as it increases the contamination by the much more numerous, less massive and less

biased haloes. The corresponding effective halo masses $M_{\rm eff}$ for the faint, bright and brightest subsamples are computed by solving the equation $b(M_{\rm eff}, z) = \langle b \rangle(z)$, which yields $M_{\rm eff} \sim 2 \times 10^{12}\, h^{-1}\, {\rm M}_{\odot}$, $\sim 3 \times 10^{12}\, h^{-1}\, {\rm M}_{\odot}$ and $\sim 10^{13}\, h^{-1}\, {\rm M}_{\odot}$, respectively, for the reference model $\langle b \rangle$ values. The central panel of Fig. 1 compares models with the same scatter $\Sigma = 0.1$ dex but different values of the duty cycle $f_{\rm opt}$, as labelled. Increasing $f_{\rm opt}$ implies mapping the same number of quasars to less numerous haloes (cf. equation 1), which are more massive and more biased, thus inducing an overall increase in the average predicted bias. Just the opposite is true if the duty cycle is decreased.

The S09 bias measurements are consistent with a constant duty cycle $f_{\rm opt} = 6 \times 10^{-4}$ and small scatter $\Sigma = 0.1$ dex, though this model is 0.5–1σ high in the faint and bright bins and 1σ low (compared to the solid circle) in the brightest bin. Allowing an increase in $f_{\rm opt}$ with increasing luminosity would slightly improve the match to the data. On the other hand, the right-hand panel of Fig. 1 shows that a model with a significantly decreasing duty cycle (dotted line), equal to $f_{\rm opt} = 6 \times 10^{-4}$ at $\log(L/{\rm erg\ s^{-1}}) = 46.31$ and to $f_{\rm opt}/2$ and $f_{\rm opt}/4$ at $\log(L/{\rm erg\ s^{-1}}) = 46.56$ and $\log(L/{\rm erg\ s^{-1}}) = 46.84$, respectively, is inconsistent with the autocorrelation bias for the highest luminosity bin at the $\sim 2\sigma$ level. However, if we take the S09 bias measurement that includes negative data points, or the cross-correlation measurement, then the discrepancy is only $\sim 1\sigma$. A model characterized by a high duty cycle and a larger scatter in the luminosity–halo relation (long-dashed line) is also consistent with the data at the $\sim 1\sigma$ level.

To make use of the full data sets available, we compute the correlation function for a subset of representative models. The solid circles with error bars in the left-hand, central and right-hand panels of Fig. 2 are the projected correlation functions $W_{\rm P}(R_{\rm P})$ estimated by S09 for the faint, bright and brightest quasar samples, respectively (the cross-correlation function is shown for the brightest sample). The solid lines in each panel refer to the prediction of the reference model discussed in Fig. 1 defined by a constant $f_{\rm opt} = 6 \times 10^{-4}$ with the correlation function computed via equation (7) by integrating over the redshift distribution of the clustering sample. We have verified that simply computing the correlation function at the mean redshift of $z = 1.45$ produces essentially the same result (the correlation function in the latter case is systematically lower by only ~3–4 per cent, at fixed $f_{\rm opt}$). The reference model agrees well with the $W_{\rm P}(R_{\rm P})$ data at $R_{\rm P} \leq 40\, h^{-1}$ Mpc. While the increases in the predicted $W_{\rm P}(R_{\rm P})$ for the bright and brightest samples are modest, they clearly improve the fit to the data relative to a luminosity-independent $W_{\rm P}(R_{\rm P})$ (dotted lines).

For the bright and brightest samples, the data at larger scales do not follow the theoretically predicted shape. Since this shape is generic to Λ cold dark matter models with scale-independent large-scale bias, and thus to models that accurately describe observed galaxy clustering at lower redshifts (e.g. Reid et al. 2010), we attribute little significance to this discrepancy at present; error bars in $w_{\rm P}(R_{\rm P})$ are correlated, and the jackknife method may underestimate them at large scales.

Other methods (see Section 4.2 below) favour duty cycles that evolve in time. The study by Shankar et al. (2009a) yields a rapidly evolving duty cycle that can be approximated as $f = f(z = 1.45) \times [(1+z)/2.45]^8$ in the range $0.5 \lesssim z \lesssim 2$ (see their fig. 7c). Applying the latter model to equations (7) yields the long-dashed lines in Fig. 2, which is very similar to the reference model computed at $z = 1.45$.

Fig. 1 demonstrates a tradeoff between $f_{\rm opt}$ and Σ: the bias decreases with either decreasing duty cycle or increasing scatter. The contours in Fig. 3 present this tradeoff systematically, showing regions in the ($f_{\rm opt}$, Σ) parameter space that are consistent with the $b(L)$ data at the 1, 2 and 3σ confidence levels. For these contours, we assume that $f_{\rm opt}$ is independent of L and compute the predicted bias at $z = 1.45$. The two parameters are not completely degenerate, as raising Σ flattens the $b(L)$ relation in addition to lowering its amplitude. If we adopt the autocorrelation estimate of $b(L)$ for the highest luminosity bin (rightmost solid circle in Fig. 1, left-hand panel of Fig. 3), then values of $\Sigma > 0.65$ are inconsistent at the 1σ level because they predict a $b(L)$ relation that is too flat. However, the lower $b(L)$ estimated from cross-correlation (open square in Fig. 1, right-hand panel of Fig. 3) allows higher Σ values, and the 2σ constraints are weak in either case. Future bias measurements with smaller uncertainties could help to break the $f_{\rm opt}$–Σ degeneracy, but only

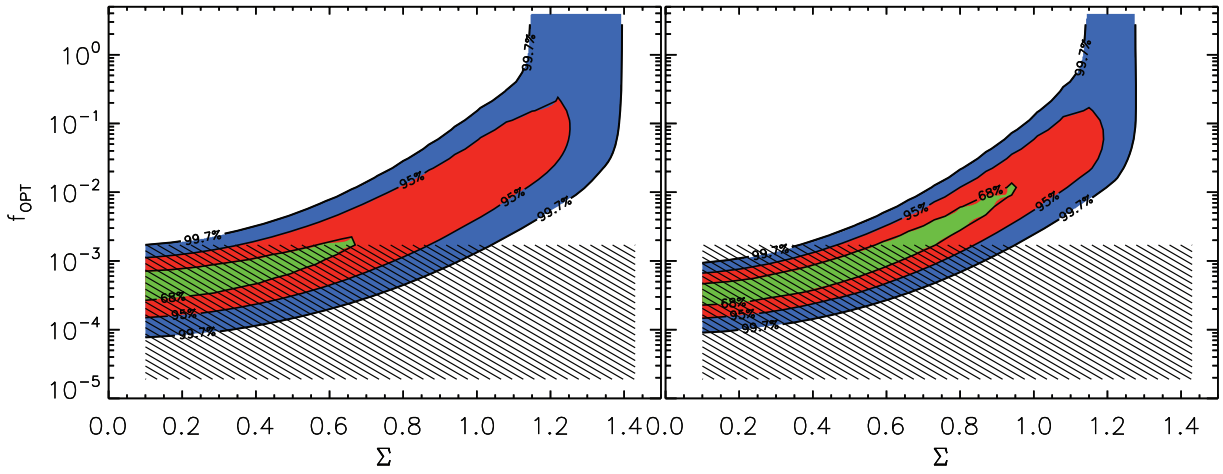

Figure 3. Constraints on the optical duty cycle $f_{\rm opt}$ and luminosity–halo mass scatter Σ derived from the $b(L)$ data points shown in Fig. 1. Contours mark the regions of parameter space with $\chi^2 = 1.0$ 4.0, and 9.0, corresponding to 68, 95 and 99.7 per cent confidence levels for one degree of freedom (three data points minus two parameters). Results in the left-hand panel adopt the autocorrelation $b(L)$ estimate for the highest luminosity bin (rightmost solid circle in Fig. 1), while results in the right-hand panel adopt the cross-correlation estimate (open square in Fig. 1), which has a lower central value and smaller error bar. In both panels, shaded regions indicate the duty cycles $f_{\rm opt} < 2 \times 10^{-3}$ that are inconsistent with the expectations from continuity-equation models of the BH population (see Section 4.2).

to the extent that they clearly demonstrate a luminosity-dependent clustering trend. For now, we turn to independent constraints on optical duty cycles derived from the observed space density of quasars and models of the underlying BH population.

4.2 Additional constraints from the BH continuity equation

A widely used method to model the accretion history of the BH population employs a continuity equation (Cavaliere, Morrison & Wood 1971; Small & Blandford 1992) to track the growth of the BH mass function that is implied by the observed quasar luminosity function. This approach is reviewed extensively by Shankar et al. (2009a; hereafter SWM), who apply it to a compilation of recent data sets, and whose results and methodology we adopt here. The parameters of a model are the radiative efficiency ϵ, which converts an observed luminosity to a corresponding mass accretion rate and the Eddington ratio $\lambda = L/L_{\rm Edd}$, which determines the mass of the BHs to be associated with a given observed luminosity. The method can be generalized to allow a distribution of λ values (Shankar 2009). For a single λ value, the duty cycle is simply

$$f(M_{\rm BH}, z) = \frac{\Phi(L, z)}{\Phi_{\rm BH}(M_{\rm BH}, z)}, \quad (8)$$

where $\Phi(L, z)$ is the quasar luminosity function and $\Phi(M_{\rm BH}, z)$ is the BH mass function at the mass that corresponds to luminosity L, $M_{\rm BH} = 10^8\ \lambda^{-1}\ (L/10^{46.1}\ {\rm erg\ s^{-1}})\ {\rm M_\odot}$. For a distribution of λ, one must take some care in defining the meaning of the term 'active'. At redshifts $z > 1$, BH mergers are expected to play a minor role in shaping $\Phi(M_{\rm BH}, z)$ relative to accretion (SWM), and we neglect them here.

The left-hand panel of Fig. 4, analogous to fig. 7c of SWM, shows the optical duty cycle as a function of BH mass at $z = 1.45$ predicted by several different continuity equation models. The model shown by the solid curve has $\lambda = 0.6$ and $\epsilon = 0.065$, independent of mass and redshift, which SWM show yields a good match to observational estimates of the local BH mass function. We convert the total duty cycle to the optical duty cycle using $f_{\rm opt} = f/3$, based on the ratio of the optical luminosity function for the SDSS quasar sample to the bolometric luminosity function in SWM. Above $M_{\rm BH} = 10^{8.8}\ {\rm M_\odot}$, the predicted duty cycle is $f_{\rm opt} = 3.6 \times 10^{-3}$, while the differing shapes of the quasar luminosity function and the evolved BH mass function imply higher duty cycles at lower masses. The thick vertical lines mark the masses that correspond to the lower luminosity limit of the S09 sample at $z = 1.45$, $\log M_{\rm BH} = 8.2 - \log\lambda$. As discussed by SWM, including BH mergers in the mass function evolution or varying the bolometric luminosity functions or bolometric corrections within observationally acceptable bounds has minimal impact on the inferred duty cycles at these redshifts; the largest systematic uncertainties are associated with the choices of λ and ϵ. The dotted curve shows a model with $\lambda = 0.3$, which has similar shape but higher normalization. The normalization trend is easily understood: the integrated quasar emissivity determines the total mass density of the BH population (Sołtan 1982), and assuming lower λ shifts this density to more massive, hence rarer, BHs, which must have a higher duty cycle to reproduce the luminosity function. The dashed curve shows a model with a *spread* in Eddington ratios, Gaussian in $\log\lambda$ with 0.6-dex dispersion and peak at $\lambda_{\rm med} = 0.3$, evolved with the techniques described in Shankar (2009). Results are intermediate between the two constant-λ models. However, in this case the S09 luminosity threshold does not correspond to a sharp mass cut, so the dot–dashed curve shows $f_{\rm opt}$ with the additional criterion that $\log\lambda > 8.2 - \log M_{\rm BH}$, which eliminates those lower mass BHs whose Eddington ratio would be too low to enter the S09 sample at $z = 1.45$. This curve is slightly jagged because the calculation uses a discrete representation of the Gaussian $\log\lambda$ distribution rather than a smooth function (see Shankar 2009).

The right-hand panel of Fig. 4 shows the optical duty cycle at $M_{\rm BH} = 10^9\ {\rm M_\odot}$ and $z = 1.45$ for models with a range of Eddington ratios and radiative efficiencies. For lower ϵ, the observed quasar emissivity implies a higher BH mass density, hence a higher space density of BHs at a given mass and thus a lower duty cycle. However, observational estimates of the local BH mass density imply $\epsilon \gtrsim 0.06$ (see SWM for extensive discussion), and arguments from accretion disc theory favour $\epsilon \approx 0.08$–0.2 depending on assumptions about typical BH spins (e.g. Berti & Volonteri 2008, and references therein). Together with observational estimates favouring Eddington ratios $\lambda \approx 0.25$ (Kollmeier et al. 2006) or even lower (e.g. Netzer & Trakhtenbrot 2007) at this luminosity and redshift, we conclude

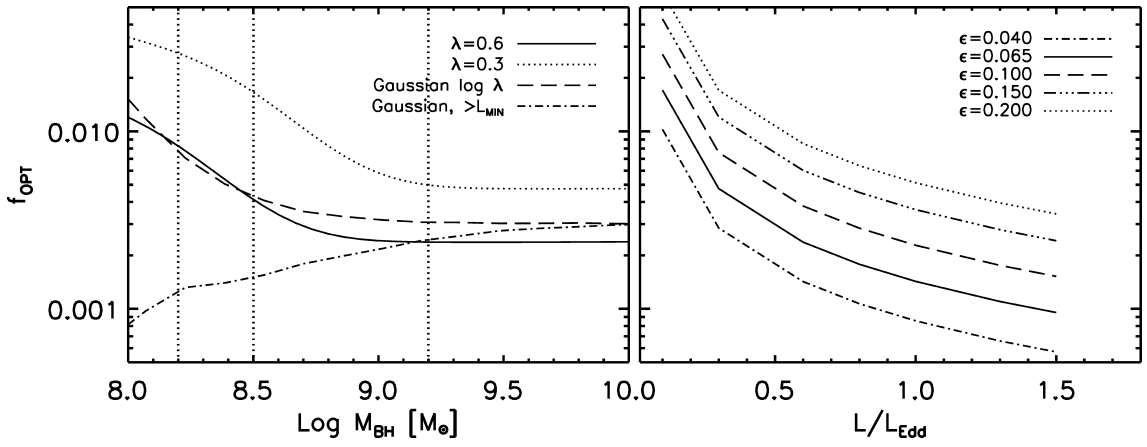

Figure 4. Optical duty cycles predicted by continuity-equation models of the BH population, as discussed in Section 4.2, including a factor of three correction for obscuration, $f_{\rm opt} = f/3$. Left: optical duty cycle versus BH mass at $z = 1.45$ for models with Eddington ratio $\lambda = 0.6$ (solid line), $\lambda = 0.3$ (dotted line) and a 0.6-dex Gaussian spread of $\log\lambda$ centred at $\lambda_{\rm med} = 0.3$ (dashed line), all assuming radiative efficiency $\epsilon = 0.065$. Thick vertical-dotted lines show the masses corresponding to the S09 sample luminosity threshold at $z = 1.45$ for $\lambda = 1.0$, 0.5, 0.1 (left to right). The dot–dashed curve shows the duty cycle in the Gaussian case with the additional requirement that the Eddington ratio is high enough to pass this luminosity threshold. Right: optical duty cycle at $M_{\rm BH} = 10^9\ {\rm M_\odot}$ and $z = 1.45$ for models with different choices of $\lambda = L/L_{\rm Edd}$ and ϵ, as indicated. Within a given model, the values of λ and ϵ have no scatter and are held fixed during evolution.

that continuity-equation models imply optical duty cycles $f_{\rm opt}(z = 1.45) > 2 \times 10^{-3}$ in the S09 luminosity range. The robustness of this lower limit depends on how pessimistically one views the systematic uncertainties in the local BH mass density (hence ϵ), direct BH mass estimates (hence λ) and obscuration fractions (hence $f_{\rm opt}/f$), but it is much easier to find ways to push $f_{\rm opt}$ higher than to push it lower.

Returning to Fig. 3, the shaded bands show the values of $f_{\rm opt} < 2 \times 10^{-3}$ excluded by the continuity equation arguments. Models consistent with this constraint and the 95 per cent constraint from the $b(L)$ data have high scatter, $\Sigma > 0.4$ dex. This conclusion holds regardless of whether we use the autocorrelation or cross-correlation estimates of the bias in the highest luminosity bins (left-hand and right-hand panels, respectively). In the right-hand panel of Fig. 1, the long-dashed line shows an explicit example of $b(L)$ for a model with $f_{\rm opt} = 2 \times 10^{-3}$ and $\Sigma = 0.5$. The prediction is very similar to that of the low-scatter model with $f_{\rm opt} = 6 \times 10^{-4}$, though the larger scatter does produce slightly flatter $b(L)$.

5 SUMMARY AND IMPLICATIONS

Studies of quasar clustering have generally failed to find any significant dependence of clustering strength on quasar luminosity, at least at $z \leq 2.5$. The S09 study is one of the first to separate luminosity dependence from redshift evolution, and it mostly confirms this basic finding, except for the $\sim 2\sigma$ increase in bias for the brightest 10 per cent of the quasars at $z \leq 2.5$. At first glance, the absence of luminosity dependence appears to contradict models like those of Martini & Weinberg (2001) or Haiman & Hui (2001), which assume a monotonic relation between quasar luminosity and host halo mass and therefore predict a stronger bias for more luminous quasars. However, Figs 1 and 2 show that the S09 results can be reproduced by a model with constant duty cycle for optical quasar activity, $f_{\rm opt} \approx 6 \times 10^{-4}$, and minimal scatter between luminosity and halo mass. The weakness of the predicted luminosity dependence arises because, even with the large size of the SDSS quasar survey, the dynamic range of luminosity at fixed redshift is not very large ($\approx$0.5 dex), and the host haloes at these luminosities and redshifts are not on the extreme, steeply rising tail of the $b(M)$ relation. Croton (2009) reaches a similar conclusion (comparing to other data sets), with a model that is different in technical implementation from ours but similar in practice.

However, the S09 bias measurements can also be fit by models with a higher duty cycle and substantial scatter between luminosity and halo mass. The increase in bias for S09's highest luminosity bin implies an upper limit on scatter, but this increase is only marginally detected depending on which method is used to estimate the bias. Fig. 1 shows an explicit example of an acceptable model with $f_{\rm opt} = 2 \times 10^{-3}$ and lognormal scatter $\Sigma = 0.5$ dex, and Fig. 3 shows the regions of the $f_{\rm opt}$–Σ parameter space that yield acceptable agreement with the S09 bias measurements. As discussed in Section 4.2, models of the quasar population that infer the duty cycle by evolving the BH mass function and comparing to the quasar luminosity function imply $f_{\rm opt} \gtrsim 2 \times 10^{-3}$. Taken together, the clustering constraints and the continuity equation models imply substantial scatter in the luminosity–halo mass relation, with $\Sigma \geq 0.4$ dex.

Applying linewidth estimators of BH mass in the AGN and Galaxy Evolution Survey (AGES), Kollmeier et al. (2006) infer a scatter in quasar Eddington ratios of $\sigma_\lambda \leq 0.3$ dex, though Netzer et al. (2007) and Shen et al. (2008) argue for somewhat larger scatter based on other data sets. The total scatter between luminosity and halo mass is a combination (in quadrature) of the scatter in Eddington ratios and the scatter between halo mass and BH mass. Physically, many models of quasar activity predict broad Eddington ratio distributions as a consequence of 'post-peak' accretion on to a central BH, after a rapid growth phase in which the BH mass grows exponentially at a near-Eddington accretion rate (e.g. Yu & Lu 2008; Hopkins & Hernquist 2009; Shen 2009). Various authors have argued that such prolonged post-peak activity is the key to reconciling the faint end of the AGN luminosity function with measurements of quasar bias at low redshift (e.g. the above papers and Lidz et al. 2006; Marulli et al. 2008; Bonoli et al. 2010; Shankar et al., in preparation). We conclude that scatter of 0.4–0.6 dex in the luminosity–halo mass relation at these redshifts is plausible on both theoretical and observational grounds.

Several groups have recently tried to measure, or limit, redshift evolution of the scaling between BH mass and host galaxy properties. As several recent papers have pointed out (e.g. Lauer et al. 2007; Shankar et al. 2009b; Shen & Kelly 2009; Merloni et al. 2010), a large scatter between quasar luminosity and the galaxy scaling property (such as stellar mass or velocity dispersion σ) can bias such measurements. These biases arise from a combination of flux-limit effects, rapidly falling stellar mass (or velocity dispersion) functions of galaxies and intrinsic scatter in the scaling relations themselves, which conspire to cause an apparent rise in the mean BH mass at fixed galaxy properties with increasing redshift. Merloni et al. (2010) note that an increasing scatter with increasing z could be enough to explain the trend of evolving BH mass over galaxy mass ratio measured in their data. Decarli et al. (2010; see also Bennert et al. 2010 for similar conclusions at lower redshifts) argue that strong evolution in the BH mass–galaxy mass relation is still present even after carefully accounting for flux-limit effects, although they did not allow the possibility of redshift-dependent scatter in the relations (see also discussion in Shen & Kelly 2009). The substantial scatter inferred from our analysis shows that biases associated with this scatter must be carefully assessed in studies of the evolution of scaling relations.

A large dispersion between quasar luminosity and host halo mass cannot be the general rule at all redshifts and luminosities. In particular, explaining the high clustering amplitude measured for SDSS quasars at $z \approx 4$ by Shen et al. (2007) requires both minimal scatter and duty cycles close to one (White et al. 2008; Bonoli et al. 2010; Shankar et al. 2009c). The quasars in this $z \approx 4$ sample are considerably more luminous than the lower redshift quasars whose clustering is modelled here, so in principle the difference in scatter could reflect either redshift dependence or luminosity dependence. Fine et al. (2008) claim direct empirical evidence for a decrease of Σ with increasing quasar luminosity, based on linewidth estimates of BH mass, and a decrease of this sort is also found in numerical simulations of merger-driven quasar activity (e.g. Hopkins & Hernquist 2009, and references therein). Assuming that $\lambda \approx 1$ sets an upper limit on BH luminosity, decreasing scatter at high luminosity is plausible because the BH mass function declines rapidly at high masses, so that the most luminous quasars will almost always be powered by BHs radiating near the maximum allowed Eddington ratio. (These arguments address only the scatter in λ, not the scatter in BH mass at fixed halo mass.) We have checked that we can fit the $b(L)$ data in Fig. 1 using models with $f_{\rm opt} \approx 10^{-3}$ and decreasing scatter at high luminosity, e.g. $\Sigma(L) = 0.6, 0.3, 0.1$ dex for the three bins of increasing luminosity, or even $\Sigma(L) = 0.4, 0.2, 0.1$ dex. However, the bias in the highest luminosity bin, which is rather uncertain at present, can significantly constrain such models.

The duty cycles inferred from our analysis at $z \approx 1.45$ are substantially lower than the values $f \approx 0.2$ and $f \approx 1$ inferred from the

Shen et al. (2007) measurements of the clustering of quasars at $z \approx 3$ and $z \approx 4$ (see Shen et al. 2007; White et al. 2008; Shankar et al. 2009c). This decline in duty cycle at low redshifts is expected from continuity equation models: the BH mass function grows in time, but the observed quasar luminosity function declines at $z < 2$, so a lower duty cycle is required to reconcile them (see, e.g. fig. 7 of SWM). Our current analysis does not constrain duty cycle evolution at $z < 2$, but strong evolution over this interval is predicted by the SWM model and is consistent with the S09 correlation function data (see Fig. 2).

The measurements in S09 provide significant constraints on the relation between quasar luminosity and halo mass, though leaving substantial degeneracy between the duty cycle and the scatter in this relation. Reducing statistical errors and remaining systematic uncertainties, especially for the brightest luminosities, would tighten these constraints; in particular, an unambiguous and precise measurement of luminosity-dependent bias would place much tighter restrictions on scatter. The quasar catalogue from SDSS DR7 (Adelman-McCarthy et al. 2008) should yield noticeable improvements, with roughly 50 per cent smaller error bars and fewer issues with internal boundaries in the survey region. Since the SDSS quasar sample has high completeness and (with DR7) covers most of the high-latitude northern sky, it will be difficult to go much further with autocorrelation measurements in the S09 luminosity and redshift range. Cross-correlation against denser samples of objects – fainter AGN or bright galaxies – could yield higher precision clustering measurements, perhaps with photometric samples from surveys such as Pan-STARRS and LSST, but perhaps requiring spectroscopic samples like those envisioned for ambitious baryon acoustic oscillation experiments. The constraints on host halo populations can also be improved by extending clustering measurements to smaller scales, where quasar pairs from the same halo contribute, and to fainter luminosities, such as those probed by the 2dF Quasar Redshift Survey, the SDSS photometric quasar catalogue and X-ray surveys (e.g. Hennawi et al. 2006; Myers et al. 2007; Plionis et al. 2008; Hennawi et al. 2009); for example, Shen et al. (2009b) use small-scale measurements to put constraints on the duty cycle of BHs in satellite galaxies. Quasar clustering as a cosmological tool has moved from a prospect (Osmer 1981) to reality, and the growing precision and dynamic range of these measurements – in luminosity, redshift and length-scale – will teach us about the growth of supermassive BHs and the mechanisms that transform them from dormant monsters to brilliant beacons and back.

ACKNOWLEDGMENTS

FS acknowledges the Alexander von Humboldt Foundation for support. FS and DW also acknowledge support from NASA Grant NNG05GH77G, and DW acknowledges support of an AMIAS membership at the Institute for Advanced Study. We thank Raul Angulo, Luca Graziani, Jeremy Tinker, Jaiyul Yoo and Zheng Zheng for interesting and helpful discussions. We thank the anonymous referee for comments that led to significant improvements of the paper.

REFERENCES

Adelman-McCarthy J. K. et al., 2007, ApJS, 172, 634
Adelman-McCarthy J. K. et al., 2008, ApJS, 175, 297
Bennert V. N., Treu T., Woo J.-H., Malkan M. A., Le Bris A., Auger M. W., Gallagher S., Blandford R. D., 2010, ApJ, 708, 1507
Berti E., Volonteri M., 2008, ApJ, 684, 822
Bonoli S., Shankar F., White S. D. M., Springel V., Wyithe J. S. B., 2010, MNRAS, 404, 399
Cattaneo A., Dekel A., Devriendt J., Guiderdoni B., Blaizot J., 2006, MNRAS, 370, 1651
Cavaliere A., Vittorini V., 2000, ApJ, 543, 599
Cavaliere A., Morrison P., Wood K., 1971, ApJ, 170, 223
Cook M., Lapi A., Granato G. L., 2009, MNRAS, 397, 534
Croton D. J., 2009, MNRAS, 394, 1109
Croton D. J. et al., 2006, MNRAS, 365, 11
Decarli R., Falomo R., Treves A., Labita M., Kotilainen J. K., Scarpa R., 2010, MNRAS, 402, 2543
Eisenstein D. J., Hu W., 1999, ApJ, 511, 5
Ferrarese L., 2002, ApJ, 578, 90
Ferrarese L., Ford H., 2005, Space Sci. Rev., 116, 523
Ferrarese L., Merritt D., 2000, ApJ, 539, L9
Fine S. et al., 2008, MNRAS, 390, 1413
Gebhardt K. et al., 2000, ApJ, 539, L13
Giocoli C., Moreno J., Sheth R. K., Tormen G., 2007, MNRAS, 376, 977
Graham A. W., 2007, MNRAS, 379, 711
Granato G. L., De Zotti G., Silva L., Bressan A., Danese L., 2004, ApJ, 600, 580
Granato G. L., Silva L., Lapi A., Shankar F., De Zotti G., Danese L., 2006, MNRAS, 368, L72
Haiman Z., Hui L., 2001, ApJ, 547, 27
Hennawi J. F. et al., 2006, AJ, 131, 1
Hennawi J. F. et al., 2009, ApJ, in press (arXiv:0908.3907)
Hopkins P. F., Hernquist L., 2009, ApJ, 698, 1550
Hopkins P. F., Hernquist L., Cox T. J., Robertson B., Di Matteo T., Springel V., 2006, ApJ, 639, 700
Hopkins P. F., Lidz A., Hernquist L., Coil A. L., Myers A. D., Cox T. J., Spergel D. N., 2007, ApJ, 662, 110
Kauffmann G., Haehnelt M., 2000, MNRAS, 311, 576
Kollmeier J. A. et al., 2006, ApJ, 648, 128
Lapi A., Shankar F., Mao J., Granato G. L., Silva L., De Zotti G., Danese L., 2006, ApJ, 650, 42
Lauer T. R., Tremaine S., Richstone D., Faber S. M., 2007, ApJ, 670, 249
Lidz A., Hopkins P. F., Cox T. J., Hernquist L., Robertson B., 2006, ApJ, 641, 41
Magorrian J. et al., 1998, AJ, 115, 2285
Malbon R. K., Baugh C. M., Frenk C. S., Lacey C. G., 2007, MNRAS, 382, 139
Marconi A., Risaliti G., Gilli R., Hunt L. K., Maiolino R., Salvati M., 2004, MNRAS, 351, 169
Martini P., Weinberg D. H., 2001, ApJ, 547, 12
Marulli F., Bonoli S., Branchini E., Moscardini L., Springel V., 2008, MNRAS, 385, 1846
Merloni A., Rudnick G., Di Matteo T., 2004, MNRAS, 354, 37
Merloni A. et al., 2010, ApJ, 708, 137
Miralda-Escudé J., Kollmeier J., 2005, ApJ, 619, 30
Monaco P., Fontanot F., Taffoni G., 2007, MNRAS, 375, 1189
Murray N., Quataert E., Thompson T. A., 2005, ApJ, 618, 569
Myers A. D., Brunner R. J., Nichol R. C., Richards G. T., Schneider D. P., Bahcall N. A., 2007, ApJ, 658, 85
Netzer H., Trakhtenbrot B., 2007, ApJ, 654, 754
Netzer H., Lira P., Trakhtenbrot B., Shemmer O., Cury I., 2007, ApJ, 671, 1256
Osmer P. S., 1981, ApJ, 247, 762
Plionis M., Rovilos M., Basilakos S., Georgantopoulos I., Bauer F., 2008, ApJ, 674, 5
Reid B. A. et al., 2010, MNRAS, 404, 60
Richards G. et al., 2006, ApJS, 166, 470
Ross N. P. et al., 2009, ApJ, 697, 1634
Salucci P., Szuszkiewicz E., Monaco P., Danese L., 1999, MNRAS, 307, 637
Schneider D. P. et al., 2007, ApJ, 134, 102
Shankar F., 2009, New Astron. Rev., 53, 57
Shankar F., Mathur S., 2007, ApJ, 660, 1051

Shankar F., Salucci P., Granato G. L., De Zotti G., Danese L., 2004, MNRAS, 354, 1020
Shankar F., Lapi A., Salucci P., De Zotti G., Danese L., 2006, ApJ, 643, 14
Shankar F., Weinberg D. H., Miralda-Escudé J., 2009a, ApJ, 690, 20 (SWM)
Shankar F., Bernardi M., Haiman Z., 2009b, ApJ, 694, 867
Shankar F., Crocce M., Miralda-Escudé J., Fosalba P., Weinberg D. H. 2009c, ApJ, in press (arXiv:0810.4919)
Shen Y. et al., 2007, AJ, 133, 2222
Shen Y., 2009, ApJ, 704, 89
Shen Y., Kelly B. C., 2010, ApJ, 713, 41
Shen Y., Greene J. E., Strauss M. A., Richards G. T., Schneider D. P., 2008, ApJ, 680, 169
Shen Y. et al., 2009a, ApJ, 697, 1656 (S09)
Shen Y. et al. 2009b, ApJ, in press (arXiv:0903.4492)
Sheth R. K., Tormen G., 1999, MNRAS, 308, 119
Sheth R., Mo H. J., Tormen G., 2001, MNRAS, 323, 1
Silk J., Rees M. J., 1998, A&A, 331, L1
Small T. A., Blandford R. D., 1992, MNRAS, 259, 725
Sołtan A., 1982, MNRAS, 200, 115
Steed A., Weinberg D. H., 2003, preprint (astro-ph/0311312)
Tundo E., Bernardi M., Hyde J. B., Sheth R. K., Pizzella A., 2007, ApJ, 663, 53
White M., Martini P., Cohn J. D., 2008, MNRAS, 390, 1179
Wyithe J. S. B., Loeb A., 2003, ApJ, 595, 614
Wyithe J. S. B., Loeb A., 2005, ApJ, 634, 910
Wyithe J. S. B., Loeb A., 2009, MNRAS, 395, 1607
York D. G. et al., 2000, AJ, 120, 1579
Yu Q., Lu Y., 2004, ApJ, 602, 603
Yu Q., Lu Y., 2008, ApJ, 689, 732
Yu Q., Tremaine S., 2002, MNRAS, 335, 965

This paper has been typeset from a TEX/LATEX file prepared by the author.